Valence selective DAFS measurements of Mn in $La_{1/3}Ca_{2/3}MnO_3$

Bruce Ravel,[a]* Stéphane Grenier,[a] Hubert Renevier[a] and Chang-Beom Eom[b]

[a]Laboratoire de Cristallographie, CNRS, BP 166, 38042 Grenoble, France, and [b]Dept. of Mech. Engineering and Mat. Sci., Duke Universty, Durham, NC 27708 USA. E-mail: ravel@phys.washington.edu

The manganese perovskite system $La_{1-x}Ca_xMnO_3$ displays a complex phase diagram of structural, magnetic, and transport properties with varying Ca concentration. At $x = 2/3$ and at low temperature, the system is antiferromagnetic with Mn^{4+} and Mn^{3+} ions occupying special positions in a charge-ordered supperlattice. The charge ordering transition at about 260 K is characterized by the appearance of satellite peaks around certain strong normal lattice reflections. The normal lattice reflections are due to scattering from planes containing Mn^{4+} and Mn^{3+} ions in nearly stoichiometric proportion, however the superlattice reflections are due to scattering from planes containing only Mn^{4+} ions. By measuring Diffraction Anomalous Fine-Structure spectra on a superlattice reflection and its associated normal lattice reflection, it is possible to isolate absorption-like spectra for the two Mn sites. Due to the weak intensity of these superlattice reflections, we were unable to obtain high quality near-edge spectra for the superlattice reflection measured. However, the data offer useful information about the local electronic structures of the two Mn ions.

Keywords: DAFS; **CMR**; **valence selectivity.**

1. Introduction

The solid solution $La_{1-x}Ca_xMnO_3$ displays a rich variety of structural, electronic, and magnetic behaviors as the Ca concentration x is varied. Of particular interest is the low-Ca region where, at low temperature, the colossal magneto-resistance (CMR) phenomenon is observed wherein the electric resistance of the material is changed by orders of magnitude by the application of an external magnetic field. (Jin *et al.*, 1994) The details of the complex phase diagram depend upon the detailed interactions of structural, electronic, and spin degrees of freedom in the material. (Pickett & Singh, 1996)

With $x = 2/3$, the system enters a charge-ordering phase at low temperature. (Radaelli *et al.*, 1999) The Ca introduced into the lattice changes the valence of nearby Mn ions from Mn^{4+} to Mn^{3+}. At low temperature, a coherent modulation of the charge is observed. For $x = 2/3$, this charge modulation is commensurate with the lattice periodicity and superlattice reflections are observed in the diffraction pattern as satellites of certain normal reflection. For example, peaks at $(\frac{2}{3}21)$ and $(\frac{4}{3}21)$ are observed about the (121) reflection.

In this paper, we describe Diffraction Anomalous Fine Structure (DAFS) measurements on $La_{1/3}Ca_{2/3}MnO_3$ designed to directly measure the local electronic structures of the Mn^{4+} and Mn^{3+} ions. As described in Section 2., the DAFS measurement exploits crystallographic sensitivity to yield independent information about different crystallographic sites. This allows us isolate the signals of the two Mn ions.

2. Experiment

The DAFS experiment measures the energy dependence of the intensity of a diffraction peak. As the energy varies through an absorption energy, the intensity varies (Sorensen *et al.*, 1994) due to the strong contribution of the complex anomalous corrections to the scattering factor of the resonant atom. Additionally, the DAFS spectrum typically displays an oscillatory fine structure above the absorption energy which is analogous to the fine structure measured in X-Ray Absorption Fine Structure (XAFS). Because different crystallographic sites contribute to a diffraction peak with different amplitudes and phases, it is possible with DAFS to isolate an absorption-like spectrum the different sites occupied by the resonant species. This is done either by selecting reflections to which only one site contributes or by exploiting phase differences between different reflections and making linear combinations of spectra.

Our DAFS measurements were made at the D2AM (Ferrer *et al.*, 1998) beamline BM2 at the European Synchrotron Radiation Facility in Grenoble France. D2AM is equipped with a high resolution monochromator, a seven-circle goniometer, and a cryostatic sample stage and so is well suited to these measurements. The DAFS measurement requires that the sample angle be changed as the energy is scanned to continuously maintain the Bragg condition. A schematic of D2AM is shown Fig. 1. The intensity of a peak is measured at each energy by integrating the area of the θ rocking curve. The level of the background is measured on each side of the rocking curve and subtracted from the integrated intensity.

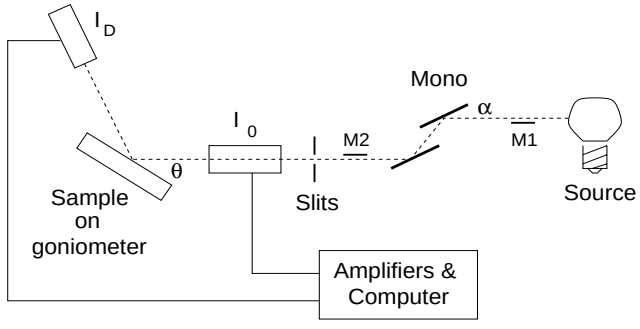

Figure 1
Schematic of the DAFS experiment at D2AM. (Ferrer *et al.*, 1998) The sample angle θ tracks the monochromator angle α to constantly maintain the Bragg condition. The mirrors M1 and M2 provide harmonic rejection and vertical focusing. Sagittal focusing is provided by the second monochromator crystal. The incident intensity is measured by passing the incident beam through a kapton foil and measuring the elastic scattering with a photodiode. The diffracted intensity of the normal lattice peak is measured with a photodiode and of superlattice peaks with a photomultiplier.

In this paper we report on DAFS measurements made on a thin film of $La_{1/3}Ca_{2/3}MnO_3$. This film was grown by pulsed laser deposition on $SrTiO_3$ substrates (Rao *et al.*, 1998; Nath *et al.*, 1999) to a thickness of about 1500 Å. At low temperature, bulk $La_{1/3}Ca_{2/3}MnO_3$ displays a charge ordering evidenced by the appearance of superlattice reflections. These reflections are consistent with a tripling of the lattice constant in one direction and an ordering of Mn^{4+} and Mn^{3+} ions. (Radaelli *et al.*, 1999) In this paper, we verify that the thin film sample displays the same charge

ordering and we report on DAFS measurements made on normal and superlattice reflections. Using these measurements, we can directly measure the Fermi energies of the two Mn ions.

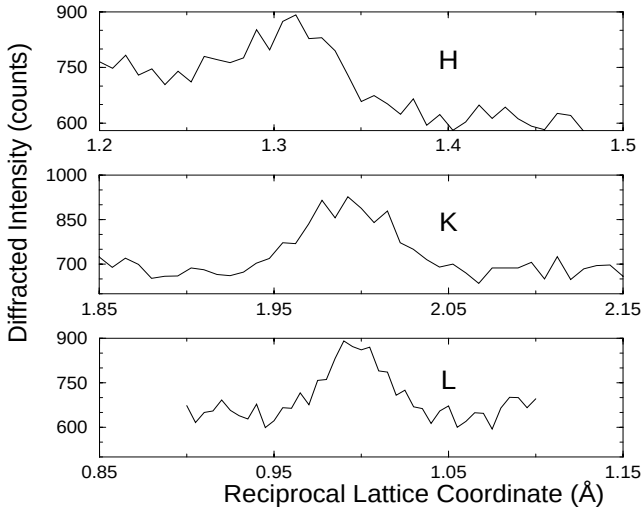

Figure 2
h-, k-, and l-scans through the ($\frac{4}{3}$21) peak at 19 K. These scans were made with one second integration time. The ($\frac{4}{3}$21) peak is absent at room temperature and the ($\frac{2}{3}$21) peak is also present at 19 K.

The presence of the superstructure was confirmed by measuring the (121), ($\frac{2}{3}$21), and ($\frac{4}{3}$21) peaks at room temperature and at 19 K. The two superlattice peaks were absent at room temperature, but were clearly visible, albeit weak, at 19 K. The ($\frac{4}{3}$21) peak is shown in Fig. 2. The charge-ordering transition is at about 260 K. (Radaelli *et al.*, 1999), so our measurements were made well within the charge-ordered phase. Data for representative scans of the (121) and ($\frac{4}{3}$21) peaks are shown in Fig. 3. The diffracted intensity normalized to the incident intensity is shown in the y-axis of Fig. 1. The scale for the (121) peak is on the left and for the ($\frac{4}{3}$21) peak on the right. The integration time for the (121) peak, however, is 2 seconds, while for the ($\frac{4}{3}$21) peak it is 200 seconds. Thus the intensity of the superlattice peak is down by 5 orders of magnitude compared to the normal peak.

3. Interpretation

The low count rate in the data and the extremely long integration time required for the measurement of the ($\frac{4}{3}$21) peak preclude the possibility of a detailed measure of the near edge structure in these DAFS data. This is unfortunate. The Diffracted Anomalous Near Edge Structure (DANES), like the X-ray Absorption Near Edge Structure (XANES) contains much information about the projected electronic densities of state of the Mn ions. With high quality DANES data and the use of appropriate theory — for example (Ankudinov *et al.*, 1998) — we could obtain detailed information about the electronic structures of the two Mn ions. The information content of the superlattice data shown in Fig. 3 is insufficient for quantitative analysis, but does provide some information about the electronic structures of the two Mn ions.

Using the crystal structure of the superlattice given in (Radaelli *et al.*, 1999), we can compute the sum $\sum \exp(i\,\vec{Q}\cdot\vec{r})$ for the Mn^{4+} and Mn^{3+} sublattices, where the sum is over all sites of each ion in the unit cell. This simple calculation tells roughly the contribution of each Mn ion to a scattering plane. For the (121) peak, we find that the Mn^{4+} and Mn^{3+} ions contribute to the diffracted intensity with a ratio of 7.987-to-4, nearly the stoichiometric proportion of 2-to-1. Thus the (121) spectrum provides information which is nearly identical to an EXAFS spectrum on this material. However for the ($\frac{4}{3}$21) peak, we find that the scattering plane contains no Mn^{3+} ions. Thus the ($\frac{4}{3}$21) peak is due to scattering from a plane containing only Mn^{4+} ions and the DAFS spectrum measured on this reflection is due entirely to the Mn^{4+} ion.

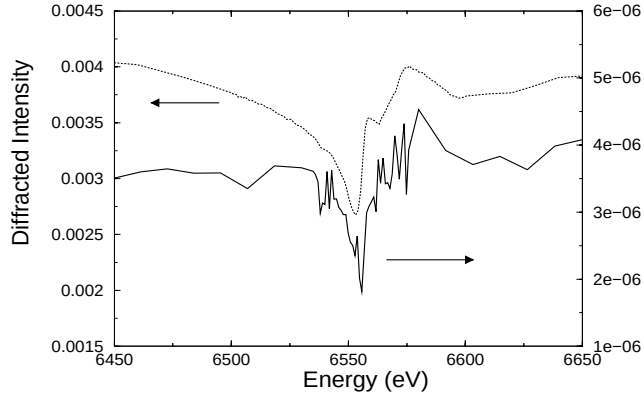

Figure 3
Data on the (121) and ($\frac{4}{3}$21) reflections at 19 K normalized to the incident intensity. The scale for the (121) peak (dashed line) is on the left and for the ($\frac{4}{3}$21) peak (solid line) on the right.

We measured 5 scans of the superlattice peak and 2 of the normal lattice peak. These 7 scans were aligned in energy using fluorescence EXAFS which was measured simultaneously with the DAFS. The minimum of the superlattice spectrum is at 6555.4(6) eV and of the normal lattice spectrum at 6553.0(2). This is a shift of 2.4(6) eV.

The bottom of the cusp is typically the minimum of $f'(E)$, the real part of the anomalous correction to the scattering factor. Because $f'(E)$ and $f''(E)$ are related by a Kramers-Krönig transform, the minimum of $f'(E)$ is near the inflection point of the main rise is $f''(E)$ and thus in $\mu(E)$ since the two functions are simply related by the optical theorem. (Cullity, 1978) Because the cusp of the ($\frac{4}{3}$21) spectrum is 2.4(6) eV higher than that of the (121) spectrum, the main rise of $f''(E)$ for the isolated Mn^{4+} ion is that amount higher than for the $f''(E)$ of the (121) spectrum.

In the (121) spectrum as in an EXAFS spectrum, a linear combination of the Mn^{4+} and Mn^{3+} is measured. Thus the main rise of the isolated Mn^{3+} $\mu(E)$ (and, equivalently, $f''(E)$) must be about 3 eV lower than for the Mn^{4+}, such that the inflection point of the combined spectrum is shifted downward by the measured amount. Thus indicated a downward shift of the local electronic density of states of the Mn^{3+} ion relative to the Mn^{4+} and a similar downward shift of the Fermi energy. This is consistent with results of total energy calculations on the $La_{1-x}Ca_xMnO_3$ system (Pickett & Singh, 1996), which predict a downward shift of about 3 eV in the Mn^{3+} total density of states.

4. Conclusion and Future Work

In this work, we have measured Mn edge DAFS on normal and superlattice reflections in $La_{1/3}Ca_{2/3}MnO_3$. From these data, we find a chemical shift of about 3 eV between the Mn^{4+} and Mn^{3+} ions. This is consistent with theoretical predictions (Pickett &

Singh, 1996) on other members of the $La_{1-x}Ca_xMnO_3$ system and is a verification of the theoretical results.

Our measurements of the $(\frac{4}{3}21)$ were limited by count rate. The low count rate and very long integration times precluded collection of high quality DANES data, although the data were sufficient for approximating the chemical shift between the Mn ions. Improving the quality of the superlattice data is essential. With a high quality $(\frac{4}{3}21)$ spectrum, the Mn^{3+} spectrum could be accurately isolated form the (121) spectrum and the chemical shift of the density of states and the Fermi energy could be precisely measured using an iterated Kramers-Krönig refinement. (Cross, 1996)

An obvious improvement to the experiment reported here would be to use a brighter source, such as an insertion device beamline at a third-generation synchrotron. A thicker sample might be useful for improving the intensity of the diffracted signal, although a significantly thicker sample would be subject to distortions due to the absorption of the sample. (Sorensen *et al.*, 1994)

DAFS was used to isolate the signal from the two Mn ions and so independently to probe their electronic structures. This powerful capability is not possible in an ordinary XAFS measurements, although similar information can often be backed out of XAFS data using empirical standards. However, direct measurements typically are more accurate and precise. The use of DAFS was made possible by the appearance of superstructure diffraction peaks at low temperature due to scattering from planes containing only Mn^{4+}. Any time that a normal or superstructural feature of a crystal provides contrast between different valence states of an element, DAFS can be used to provide site-separation as presented in this article.

One of us (BR) would like to thank the Centre Nationale de la Recherche Scientifique for financial support. We thank J.-F. Berar and S. Arnaud for experimental support at D2AM.

References

Ankudinov, A., Ravel, B., Rehr, J. & Conradson, S. (1998). *Phys. Rev. B*, **58**(12), 7565–7576.

Cross, J. (1996). *Analysis of Diffraction Anomalous Fine Structure*. Ph.D. thesis, University of Washington.

Cullity, B. (1978). *Elements of X-Ray Diffraction*. New York: Addison–Wesley, 2nd ed.

Ferrer, J. L., Simon, J. P., Berar, J. F. *et al.* (1998). *J. Synchrotron Rad.* **5**, 1346–1356.

Jin, S., Tiefel, T. H., McCormick, M., Fastnacht, R. A., Ramesh, R. & Chen, L. H. (1994). *Science*, **264**, 413–415.

Nath, T. K., Rao, R. A., Lavric, D., Eom, C., Wu, L. & Tsui, F. (1999). *Appl. Phys. Lett.* **74**, 1615.

Pickett, W. E. & Singh, D. J. (1996). *Phys. Rev. B*, **53**(3), 1146–1160.

Radaelli, P. G., Cox, D. E., Capogna, L., Cheong, S.-W. & Marezio, M. (1999). *Phys. Rev. B*, **59**(22), 14440–14450.

Rao, R. A., Lavric, D., Nath, T. K., Eom, C., Wu, L. & Tsui, F. (1998). *Appl. Phys. Lett.* **73**, 3294.

Sorensen, L., Cross, J., Newville, M., Ravel, B., Rehr, J., Stragier, H., Bouldin, C. & Woicik, J. (1994). In *Resonant Anomalous X-ray Scattering: Theory and Applications*, edited by G. Materlik, C. Sparks & K. Fischer. Amsterdam: North Holland.